Laser-modulated colloids*

H. R. KRISHNAMURTHY
Department of Physics, Indian Institute of Science, Bangalore 560 012, and Jawaharlal Nehru Centre for Advanced Scientific Research (JNCASR), Jakkur, Bangalore 560 064, India

Abstract

Interesting phenomena encountered in laser-modulated colloids and recent progress in understanding them using density functional theory and simulational studies are reviewed. Modulation of colloids by confinement, and other open questions are briefly touched on.

Keywords: Laser-modulated colloids, laser-induced freezing, density functional theory, Monte-Carlo simulations of colloids.

1. Introduction

Colloidal suspensions[1] are systems of particles in solvents, with sizes much larger than atomic dimensions but still small enough that Brownian motion prevents their sedimentation due to gravity. Laser-modulated colloids are obtained by subjecting colloidal suspensions to standing wave patterns of an electromagnetic field obtained by interfering laser beams[2–4].

The specific colloidal system[1] that I will consider in this talk consists of polyballs, which are spheres of entangled polystyrene chains, with a typical diameter $2R$ in the range 0.1–1 μ. When suspended in water, the –KSO$_4$ end groups sticking out at the surface dissociate, leaving each polyball with a large negative charge Z^*e (~1000 e). The cations released from the polyball and other (for example, salt) ions present in the solvent screen the Coulomb interaction between the polyballs, leading to an effective interaction, called the DLVO potential, given by[1]

$$V(r) = \frac{(Z^*e)^2}{\varepsilon}\left(\frac{\exp(\kappa R)}{1+\kappa R}\right)^2 \frac{\exp(-\kappa r)}{r}. \tag{1}$$

Here κ, the inverse (Debye) screening length, is given by:

$$\kappa^2 = \frac{4\pi}{\varepsilon k_B T}\left[(n_p Z^*)e^2 + \sum_\alpha n_\alpha (z_\alpha e)^2\right] \tag{2}$$

where n_p is the number density of the polyballs, and n_α, the number density of ions of type α with charge z_α which contributes to screening in addition to counterions.
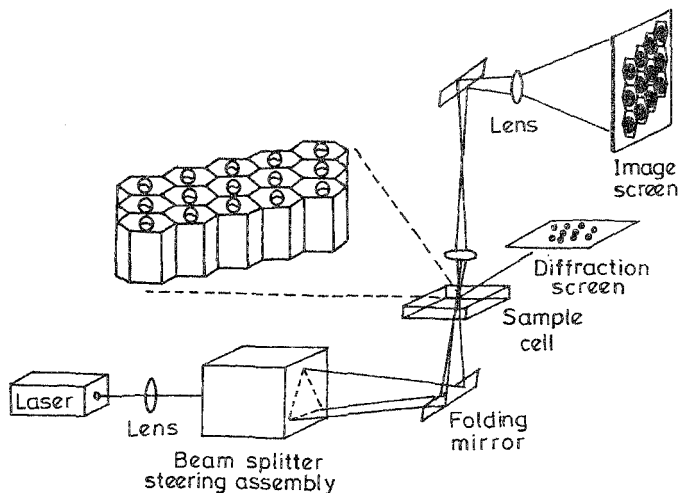
FIG. 1. Schematic diagram of the experimental setup used for studies of laser-modulated colloids (after Burns *et al*[2]).

The crucial feature of the polyball system which makes it a wonderful experimental system is the fact that κ can be tuned easily by changing the salt concentration in the solvent or the volume fraction of the polyballs: thus one can drive the system from a weakly interacting ($\kappa a_s \gg 1$, where a_s in the interparticle spacing) regime to a strongly interacting (small κa_s) regime. It is known[1] that in this process one can get phase transitions between liquid and crystalline (both bcc and fcc) phases of the colloidal system. One can even produce glassy phases with mixtures of polyballs of different sizes[1]. Subjecting the system to laser modulations with wavelength about a_s leads to fascinating ordered structures of the polyballs, dubbed[2] 'optical matter'.

The typical experimental setup for generating optical matter is shown[2] in Fig.1. The dielectric susceptibility χ of the polyballs, given by the expression[2] $\left[\left(n_1^2 - n_2^2 \right) \middle/ \left(n_1^2 / n_2^2 + 2 \right) \right] R^3$, where n_1 and n_2 are, respectively, the refractive indices of the polyballs (~ 1.58) and water (1.33), is large. The electric field of the laser modulation hence induces large dipole moments on the polyballs, leading to an effective potential $V_e(r_1) = -\frac{1}{2} \chi \left[E(r_1) \right]^2$ on the ball (with its centre) at $r_1 \cdot V_e$ is easily tuned to be compara-

ble to or larger than the thermal or interaction energies. The ordered structures of optical matter[2] then arise because the colloidal particles prefer to sit at the maxima of $[E(r)]^2$. At the simplest level, for a potential of the form

$$V_e(r_1) = \sum_i \widetilde{V}_e\big[g_i^{(f)}\big] \exp\big[i g_i^{(f)} \cdot r\big] \tag{3}$$

one will have an induced linear response in the density of the colloid given by

$$\delta\rho(r_1) = \sum_i S_{g_i^{(f)}} \widetilde{V}_e\big[g_i^{(f)}\big] \exp\big[i g_i^{(f)} \cdot r\big] \tag{4}$$

where S_q is the structure factor of the polyball liquid. Thus, the polyball liquid develops modulations that mimic the potential. But more interesting is the nonlinear response that one can generate in the presence of a strong V_e, strong correlations in the liquid, and a tuning of $(g_i^{(f)})$ to the first peak of S_q so that $S_{g_i^{(f)}}$ is large. A typical example of such a response is the phenomenon of laser-induced freezing which I discuss next.

2. Laser-induced freezing (LIF)

The phenomenon of LIF was first demonstrated by Chowdhury *et al.*[3] They subjected a 2-D polyball system (obtained by constraining the polyball system between glass plates such that only one layer of polyballs can be accommodated) to a 1-D laser modulation, with wave vectors $g_i^{(f)} = \pm q_0(0, 1)$, with q_o tuned to be at the first peak of the structure factor S_q for the 2-D polyball liquid. They were able to demonstrate that turning on the 1-D modulated V_e generated a freezing of the polyball liquid into a 2-D triangular lattice.

It is not hard to understand this phenomenon as a nonlinear response in the context of a Landau–Alexander–Mctague theory[5,6]. In this theory the difference between the free energies of the liquid and the crystalline phases is expressed as a truncated power series in terms of the Fourier components of the order parameters at the smallest six reciprocal-lattice vectors of the triangular lattice (see inset of Fig. 2). One has, by symmetry, $\rho_1 = \rho_4$, $\rho_2 = \rho_3 = \rho_5 = \rho_6$. Hence,

$$\Delta F = A\left(\rho_1^2 + 2\rho_2^2\right) + B\rho_1\rho_2^2 + C\left(\rho_1^2 + 2\rho_2^2\right)^2 + D\left(\rho_1^4 + 2\rho_2^4\right) - 2\widetilde{V}_e\rho_1 \tag{5}$$

where the tuning of the wave vector of V_e to q_o makes it couple directly to the order parameter(s) ρ_1 (and ρ_4). For a typical set of parameters, $B = -1$, $C = 1/2$, $D = 3/2$, when $V_e = 0$, as A decreases there is a first-order transition from the liquid phase (with $\rho_1 = 0$) to the crystalline phase (with $\rho_1 = \rho_2 \neq 0$) at $A \cong 0.04$. The full phase diagram obtained by minimising ΔF is shown in Fig. 2. The transition is continuous for large V_e, which makes for a very interesting phase transition. However, while later studies by Loudiyi and Ackerson[4] using direct observation and Monte Carlo simulations confirmed LIF, the nature of the transition was not explored carefully.
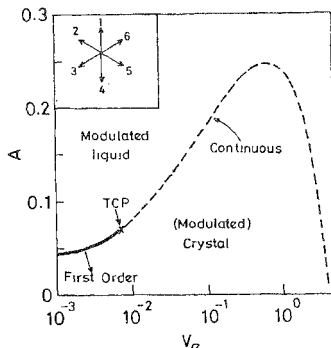
Fig. 2. Phase diagram in the Landau–Alexander–Mctague theory. In the modulated liquid phase, $\rho_1 \neq 0$, $\rho_2 = 0$. In the (modulated) crystal phase $\rho_1 \neq \rho_2 \neq 0$. Full line indicates a line of first-order transitions, and the dashed line a line of continuous transitions. TCP, the tricritical point marked by x, separates the two. *Inset*: The smallest size rlv of the triangular lattice labelled 1–6. The modulation V_e has wave vectors g_1 and $g_4 = -g_1$. Then, by symmetry, $\rho_1 = \rho_4$, $\rho_2 = \rho_3 = \rho_5 = \rho_6$.

3. Density functional theory (DFT) of laser-induced freezing

The DFT of freezing, pioneered by Ramakrishnan and Yussouff[7], has been extensively used[8] to study a variety of phenomena associated with the freezing of liquids, including defects in crystals[9], solid–solid interfaces[10], phonons[11], etc. It has also been used, with considerable success, to understand/predict the phase diagram of the colloidal system from first principles[12,13]. So it is natural to attempt to describe LIF using this framework. Earlier work in this direction[14,15], using DFT plus the nonoverlapping Guassian approximation for describing the periodic density modulations in the crystal, reached wrong conclusions about the continuous liquid → crystal transition suggested by the work of Chowdhury *et al.*[3] The conclusion was that "the symmetry gap between the fluid and the solid can never be bridged completely by the external constraint unless," (trivially,) "the external potential has the full symmetry of the solid."

We have developed[16,17] recently a DFT of LIF without uncontrolled approximations. We have shown definitively that, in the presence of an external potential V_e of lower symmetry than the crystal, the transition from the modulated liquid to the (modulated) crystal can be made to change from first order to continuous with increasing V_e *via* a tricritical point (TCP); but this happens only when a certain criterion (see later part) is satisfied by the wave vectors of V_e. The wrong conclusion in the earlier work[14,15] was reached because the choice of the wave vectors of V_e used did not satisfy this criterion. Our DFT is not bound by the limitations of the Landau–Alexander–Mctague theory (which, furthermore, as is clear from Fig. 2, has no stable crystalline phase for large V_e). In addition, our DFT is a first principles theory. We have used it (see later part) to predict the parameters for the TCP and for obtaining continuous modulated liquid → bcc crystal transitions in the context of a 3-D colloid, subject to a carefully chosen 2-D modulation.

To get a flavour of our DFT, it is enough to consider a simple version, where the order parameters ξ_G, given by the Fourier components of the 'molecular field'

$\xi(r) \equiv \ln[\rho(r)/\rho_l]$ where $\rho(r)$ is the periodic density in the modulated liquid or the crystal, are determined by minimising the free energy given (in the incompressible limit) by[7, 8]

$$\beta(F - F_l) \simeq -\ln\Phi + \sum_{G \neq 0} \frac{\xi_G^2}{2c_G^{(2)}} + \sum_{G \neq 0} \frac{\xi_G \beta \widetilde{V}_G}{c_G^{(2)}} \qquad (6)$$

where

$$\Phi \equiv \frac{1}{v_o} \int_r^{\text{cell}} \exp\left[\sum_{G \neq 0} \xi_G e^{i.G.r}\right] \equiv \frac{1}{v_o} \int_r^{\text{cell}} \exp\left[\xi(r)\right]. \qquad (7)$$

Here $\{G\}$ are the reciprocal lattice vectors (rlv) of the crystal, and $c_G^{(2)}$ is the direct correlation function of the liquid at G. The self-consistent equations for the order parameters obtained by minimising F, namely,

$$\left[\xi_G + \beta \widetilde{V}_G\right] / c_G^{(2)} = \int_r e^{iG.r} e^{\xi(r)} \Big/ \int_r e^{\xi(r)}, \qquad (8)$$

can be solved essentially exactly numerically for any finite set of order parameters, even if large, using a technique developed by us[13, 17]. Note that even if $\{\xi_G\}$ is a finite set, all the Fourier components ρ_G of $\rho(r)$, namely, $\rho_G = \int e^{iG.r} e^{\xi(r)}$, are nonzero.

For purposes of understanding the essential physics of LIF in 2-D it is enough to further simplify the theory by keeping only $c_{q_0}^{(2)} \equiv c_1^{(2)}$, *i.e.*, retain the order parameters only for the smallest set of rlv. As is known[18], the 2-D liquid freezes into a triangular lattice when $V_e = 0$ with the smallest set of rlv given by $\{g_i^{(0)}\} = \{(0, \pm 1)q_0, \left(\pm\sqrt{\frac{3}{2}}, \pm\frac{1}{2}q_0\right)$. Now, consider a 1-D modulated V_c with wave vectors $\{g_i^{(f)}\} \equiv \{(0, \pm 1)q_0\}$. Then the order parameters $\xi_{g_i^{(0)}}$ assume, by symmetry, only two values, ξ_f for the $n_f (= 2)$ vectors of the set $\{g_i^{(f)}\}$, and ξ_d for the $n_d (= 4)$ vectors of the complementary set $\{g_i^{(d)}\} \equiv \{g_i^{(0)}\} - \{g_i^{(f)}\}$. The free energy becomes

$$\beta F = -\ln[\Phi] + \frac{1}{2c_1^{(2)}}\left[n_f \xi_f^2 + n_d \xi_d^2\right] + \frac{n_f \xi_f}{c_1^{(2)}} \cdot \beta \widetilde{V}_c \qquad (9)$$

with

$$\Phi = v_0^{-1} \int_r \exp\left[\xi_f \phi_f(r) + \xi_d \phi_d(r)\right] \qquad (10)$$

where, $\phi_f(r) \equiv \sum_j \exp\left[ig_j^{(f)}.r\right]$ and $\phi_d(r) \equiv \sum_j \exp\left[ig_j^{(d)}.r\right]$. Minimising this and solving the resulting self-consistent equations, one gets the phase diagram[16,17] shown in Fig. 3. There are two phases: (i) the modulated liquid with $\xi_f \neq 0$ but $\xi_d = 0$, and (ii) the
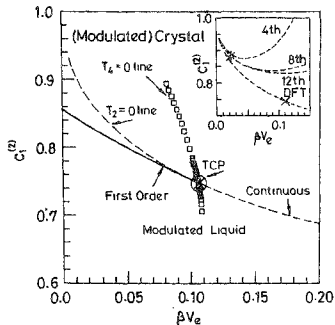
FIG. 3. DFT phase diagram of a (incompressible) 2-D system subjected to 1-D modulation, showing first-order (solid line) and continuous (dashed line) modulated liquid → crystal transitions. These are separated by the tricritical point (TCP), which is the intersection of the $T_2 = 0$ line and $T_4 = 0$ line (see text). *Inset:* $T_2 = 0$ lines of the truncated Landau thories and that of the DFT. The TCPs are marked by + (fourth-order truncation), * (8th- and 12th-order truncations), and × (full DFT).

(modulated) crystalline phase with $\xi_f \neq \xi_d \neq 0$. As is known[18], for $V_e = 0$, the liquid → crystal transition is first order and takes place at $c_1^{(2)} = 0.857$ (which corresponds to the first peak height of the liquid structure factor $S_{max} = 7.14$). When V_e is turned on, the transition remains first order, but moves to smaller values of $c_1^{(2)}$, as indicated by the solid line in Fig. 3. Thus V_e facilitates the liquid–crystal transition, which is the phenomenon of laser-induced freezing. This transition is characterized by a discontinuous change in ξ_f as well as by a discontinuous development of ξ_d. However, the jumps in ξ_d and ξ_f decrease with increasing V_e and finally vanish at the TCP given by $\beta V_e \cong 0.106$ and $c_1^{(2)} \cong 0.748$. Thereafter, one has a continuous transition from the modulated liquid to the (modulated) crystalline phase across the dashed line in Fig. 3. Qualitatively similar results are predicted by our theory for a 3-D colloid, where, when $V_e = 0$, the liquid freezes into a bcc crystal with the smallest rlv given by $\left\{ g_i^{(0)} \right\} = \left\{ (\pm 1, \pm 1, 0) q_0 / \sqrt{2}, (0, \pm 1, \pm 1,) q_0 / \sqrt{2}, (\pm 1, 0 \pm 1,) q_0 / \sqrt{2} \right\}$. Now, if one turns on a 2-D modulation with wave vectors chosen to be $\left\{ g_i^{(f)} \right\} = \left\{ (\pm 1, \pm 1, 0) q_o / \sqrt{2} \right\}$, one gets a phase diagram qualitatively similar to Fig. 3 with the TCP at $\beta V_e \cong 0.22$, $c_1^{(2)} \cong 0.55$.

The general criterion for obtaining a TCP, and a phase diagram similar to that in Fig. 3 is that[16,17] *the wave vectors of V_e must be so chosen that any odd combination of vectors of the set $\left\{ g_i^{(d)} \right\} \equiv \left\{ g_i^{(0)} \right\} - \left\{ g_i^{(f)} \right\}$ cannot be written as an integer combination of vectors of the set $\left\{ g_i^{(f)} \right\}$.*

For, if this criterion is satisfied, it can be verified easily by expanding the $\ln \Phi$ term in (9) that the Landau expansion for βF in powers of ξ_d, given $\xi_f \neq 0$ (with ξ_f treated nonperturbatively), has only even powers of ξ_d; the coefficients, which we can compute

numerically, are functions of βV_e and $c_1^{(2)}$. As $c_1^{(2)}$ and βV_e increase, the coefficient of the second-order term in this Landau expansion, T_2, changes sign and becomes negative, leading to an instability with respect to the formation of ξ_d. In the region of the parameter space where the fourth-order coefficient, T_4, is negative (but T_6 is positive), the continuous transition is preempted by a first-order transition. The TCP thus arises when both T_2 and T_4 become zero. In the 2-D case, corresponding to Fig. 3, we also show in the figure the lines along which $T_2 = 0$ (marked by dashes) and $T_4 = 0$ (marked by small squares). To the left of the $T_4 = 0$ line, where T_4 is negative, the first-order transition (solid line) preempts the continuous transition. The $T_4 = 0$ line meets the $T_2 = 0$ line at the tricritical point. In this way we obtain the precise location of the tricritical points quoted earlier. It is easy to verify that the above criterion is satisfied in the context of the modulations that we use. Note in particular that in the 3-D bcc case, a 1-D set or any arbitrary 2-D set for $\left\{ g_i^{(f)} \right\}$ picked out from $\left\{ g_i^{(0)} \right\}$ would not satisfy the above criterion.

It is interesting at this point to compare the above phase diagram with that obtainable in the Landau–Alexander–Mctague theory[3,5,6]. For this purpose we expanded the conventional Ramakrishnan–Yussouff[7,8] density functional free energy in powers of the Fourier components of $\rho(r)/\rho_0$ for the wave vectors $\left\{ g_i^{(f)} \right\}$ and $\left\{ g_i^{(d)} \right\}$ in the 2-D context. We truncated the power series at different powers and found the phase diagram by minimizing the resulting free energy. We studied truncations up to the 12th order with the results shown in the inset of Fig. 3. In each of these cases we obtain a TCP as marked; however, the numbers are very different from, and converge very slowly to, those of the full density functional theory. More importantly, the continuous transition line eventually bends upwards for large enough V_e, indicating that there is no stable crystal phase for large V_e in these truncated Landau theories, as is also clear from Fig. 2. This is in contrast to the DFT result, where the critical line asymptotes to $c_1^{(2)} \cong 0.5$ for large βV_e.

We have also shown that if the above-stated criterion on the wave vectors of V_e is satisfied, the TCP and the phase diagram are then robust with respect to the inclusion of more order parameters and of the effects of compressibility. For a more detailed discussion refer to Chakrabarti et al.[16] and Chakrabarti[17].

Finally, I would like to draw attention to our DFT calculation of laser-induced freezing in a real colloidal. For this purpose, we considered the same experimental system as Monovoukas and Gast[20] for which the DFT phase diagram is known[1] in the absence of V_e. The liquid-state DCF for this system of charged colloidal particles with diameter 1334 Å and surface charge 880 e was obtained using the rescaled mean spherical approximation of Hansen and Hayter[21,12] for the model DLVO potential in eqn (1). We focused our attention on the portion of the phase diagram where there is a first-order transition from the liquid to a bcc phase in the absence of V_e. We took the modulation wave vectors $\left\{ g_i^{(f)} \right\}$ of the external potential to be along $(\pm 1, \pm 1, 0)q_0/\sqrt{2}$ as stated above. We did calculations retaining order parameters corresponding to 10, 20, and 50
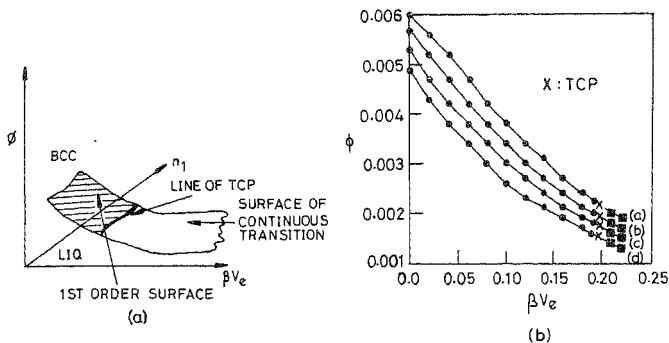
FIG. 4. (a) Schematic phase diagram of a realistic polyball suspension in the presence of an external potential (b) Phase diagram for a realistic polyball suspension in the ϕ–βV_e plane for various values of n_i. The solid line joining the open squares is the 1st order line and that joining the filled circles is the continuous transition line. TCP denotes the tricritical point.

shells of the RLVs of the bcc lattice. We retained the three-body terms[7,8] in the DFT in the same spirit of Sengupta et al.[12] with $c^{(3)} = 0.23$. In the 3-D parameter space of impurity concentration n_i, volume fraction ϕ, and βV_e, the first-order and continuous transitions between the modulated liquid and the crystal now take place across surfaces, which meet in a line of TCP, as indicated schematically in Fig. 4a. We find that in the n_i range of $(1.8–2.6) \times 10^{-9}$ mole/cm^3, βV_e is almost a constant ~0.198 along the tricritical line, as shown in Fig. 4b (compared with $\beta V_e = 0.22$ obtained in the simplest theory).

4. Monte Carlo (MC) simulations of laser-modulated colloids

We have verified many of our conclusions discussed above using MC simulation studies of laser-modulated colloids, but also obtained some surprising and interesting differences[17,19]. The simulations were conventional equilibrium MC simulations of 2-D polyballs with $2R = 1.07$ μ, $n_p = 1.81 \times 10^7$/cm^2. The inter-ball potential was of the DLVO form with $\varepsilon = 78$, $Z^* = 7800$ e. The laser-modulation potential was chosen to be $\widetilde{V}_e \cos(q_o x)$ with $q_o = 2\pi / \left(a_s \sqrt{3/2}\right)$. The simulations were done in a $\frac{\sqrt{3}}{2} L a_s \times \{L a_s\}$ cell with periodic boundary conditions for $L = 6, 8, 10, 12$ and 20, i.e., for $N = 36, 64, 100, 144$ and 400 particles, with a (randomly distorted) triangular lattice as the starting configuration.

The results obtained[17,19] for the phase diagram in the $(\kappa a_s)^{-1}$, βV_e plane are shown in Fig. 5. For $\beta V_e \lesssim 0.2$, the modulated liquid-to-crystal transition is first order, and takes
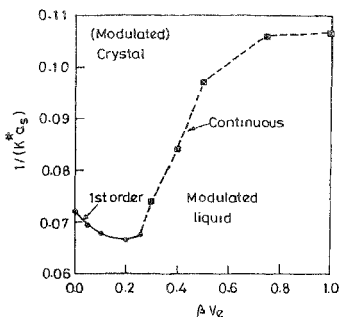
FIG. 5. The phase diagram in the $[(\kappa^* a_s)^{-1}, \beta V_e]$ plane obtained from simulations. Filled circles denote first-order transition points and the filled squares a continuous transition points.

place at a higher κa_s [lower $(\kappa a_s)^{-1}$] for increasing βV_e. This is clearly the phenomenon of LIF. For higher values of βV_e, however, the transition line bends back to lower (κa_s) [higher $(\kappa a_s)^{-1}$] values, i.e., to larger interaction strengths eventually saturating around $(\kappa a_s)^{-1} \simeq 0.11$. The transition is also continuous for $\beta V_e \geq 0.25$. The existence of a cross-over from first order to continuous transition with increasing βV_e, and the stability of the crystalline phase for large $(\kappa a_s)^{-1}$, no matter how large βV_e is, are clearly consistent with our DFT results.

However, there are two novel aspects to the simulational phase diagram (Fig. 5) as compared to the DFT phase diagram (Fig. 3). First, for $.11 > (\kappa a_s)^{-1} > .092$, as βV_e increases one gets a *laser-induced melting* (LIM) transition! Second, for $0.066 < (\kappa a_s)^{-1} < .072$, LIF is followed by an LIM transition to a reentrant-modulated liquid phase! These very interesting features deserve to be further explored using experimental, simulational and theoretical studies.

5. Modulation of colloids by confinement

There are other interesting ways to modulate colloids than by using lasers; for example, by confining it between two glass plates with repulsive charges on them. This leads to a layering phenomenon[22] as the separation between the glass plates is decreased. The tendency is especially strong when the separation is a (small) integral multiple of the mean interparticle spacing a_s, as sketched schematically in Fig. 6. But each layer can be liquid like within the layer for large κa_s (weak correlations between the particles.) For small κa_s, i.e., strong correlations, by analogy with what we have discussed, it seems clear that layering should be able to induce crystalline order within the layers. This should result in a complicated and fascinating interplay between various competing ordering tendencies. Some glimpses of the possibilities are already clear in the work of Pieranski et al.[23] where, in a wedge geometry, as a function of the separation the layers show alternately triangular and square ordering: $0 \rightarrow 1\Delta \rightarrow 2 \square \rightarrow 2\Delta \rightarrow .... \rightarrow n\Delta \rightarrow (n+1) \square \rightarrow (n+1)$
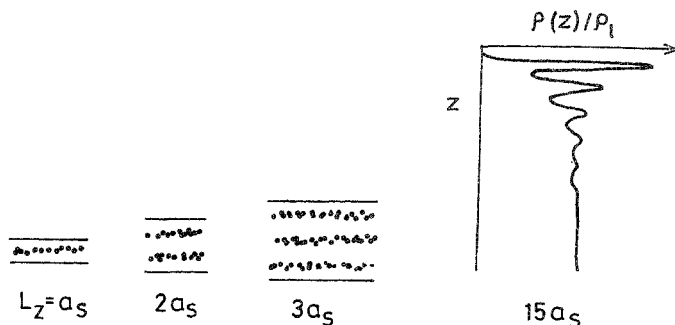
FIG. 6. Schematic diagram depicting the layering effects in a colloidal system confined between two glass plates.

$\Delta \rightarrow$ .... These phenomena need to be explored in much greater detail both experimentally and theoretically.

6. Concluding remarks

I conclude by mentioning other interesting issues in this area which I think are worth exploring in future research projects. The first obvious set of questions are about the critical phenomena associated with the continuous modulated liquid $\rightarrow$ crystal transition, in particular, its universality class. Of particular interest is light scattering from modulated colloids, especially the nature of the critical opalescence that will occur near the continuous transition from the modulated liquid to the crystal. Also for the 2-D case, complications arising from the two-dimensionality and the role of topological defects in this transition should be of interest. Another, largely unexplored class of phenomena has to do with quasiperiodic, incommensurate or random modulations. For example, can one get LIF (*i.e.*, using laser modulations of lower dimensionality) into a quasicrystal? Specifically, can a 1-D modulation with $g_n^{(f)} = \{(\pm 1, 0)q_o \tau (\pm 1, 0)q_0 / \tau\}$, where $\tau \equiv \dfrac{\sqrt{5}+1}{2}$, induce LIF into a pentagonal quasicrystal? Preliminary results from a Landau–Alexander–Mctague theory suggest that the answer is yes[24]; clearly this needs further exploring. Finally, there would be many interesting dynamical effects associated with the continuous liquid $\rightarrow$ crystal transition that would be worth exploring.

Acknowledgements

here were provided by the facilities at SERC, Indian Institute of Science and the Computer lab at JNCASR.

References

1. SOOD, A. K.
In *Solid state physics* (E. Ehrenreich and D. Turnbull, eds), Vol. 51, p.1, 1991, Academic Press, and references cited therein.

2. BURNS, M. M., FOURNIER, J. M. AND GOLOVCHENKO, J. A.
Science, 1990, **249**, 749.

3. CHOWDHURY, A., ACKERSON, B. AND CLARK, N. A.
Phys. Rev. Lett., 1985, **55**, 833.

4. LOUDIYI, K. AND ACKERSON, B. J.
Physica A, 1992, **184**, 26.

5. ALEXANDER, S. AND MCTAGUE, J.
Phys. Rev. Lett, 1978, **41**, 702.

6. LANDAU, L. D. AND LIFSHITZ, E. M.
Statistical physics. Course of theoretical physics, Vol. 5, Part 1, 3rd edn, 1985, Pegamon Press.

7. RAMAKRISHNAN, T. V. AND YUSSOUFF, M.
Phys Rev B, 1979, **19**, 2775.

8. SINGH, Y.
Phys. Rep., 1991, **207**, 351, and references cited therein.

9. RAJ LAKSHMI, M., KRISHNAMURTHY, H. R. AND RAMAKRISHNAN, T. V.
Phys. Rev. B, 1988, **37**, 1936.

10. SENGUPTA, S., KRISHNAMURTHY, H. R. AND RAMAKRISHNAN, T. V.
Europhys. Lett., 1994, **27**, 587.

11. MAHATO, M. C., KRISHNAMURTHY, H. R. AND RAMAKRISHNAN, T. V.
Phys Rev. A, 1991, **43**, 4355.

12. SENGUPTA, S. AND SOOD, A. K.
Phys. Rev. A, 1991, **44**, 1233.

13. SENGUPTA, S.
Studies in the density functional theory of freezing, Ph. D. Thesis, Indian Institute of Science, Bangalore 560 012, India, 1991.

14. XU, H. AND BAUS, M.
Phys. Lett. A, 1986, **117**, 127.

15. BARRAT, J. L. AND XU, H. J.
J. Phys.. Condens. Matter, 1990, **2**, 9445.

16. CHAKRABARTI, J., KRISHNAMURTHY, H. R. AND SOOD, A. K.
Phys Rev. Lett, 1994, **73**, 2923.

17. CHAKRABARTI, J.
Density functional and computer simulation studies of colloidal suspensions, Ph. D. Thesis, Indian Institute of Science, Bangalore 560 012, India, 1994.

18. RAMAKRISHNAN, T. V.
Phys Rev. Lett., 1982, **48**, 541.

19. CHAKRABARTI, J., KRISHNAMURTHY, H. R. AND SOOD, A. K.
Phys. Rev. Lett., 1995, **75**, 2232.

20. MONOVOUKAS, Y. AND GAST, A. P.
J. Colloid Interface Sci., 1989, **128**, 533.

21. HANSEN, J. P. AND HAYTER, J. B.
Mol Phys., 1982, **25**, 651.

22. FEHR, T. AND LOWEN, H.
Phys Rev. E, 1995, **52**, 4016, and references cited therein.

23. PIERRANSKI, P., STREZELECKI, L. AND PANSU, B.
Phys Rev Lett., 1983, **50**, 900.

24. CHINMAY DAS AND KRISHNAMURTHY, H. R.
Laser-induced freezing of a colloid into decagonal quasi-crystal, unpublished.